The Crucial Role of the K^+-Aluminium Oxide Interaction in K^+-Promoted Alumina- and Hydrotalcite-Based Materials for CO_2 sorption at High Temperatures

S. Walspurger, L. Boels, P.D. Cobden, G.D. Elzinga, W.G. Haije and R.W. van den Brink

Published in ChemSusChem 2008, 1, 643-650

September 2008

Revisions		
A		
B		
Made by: S. Walspurger	Approved: R.W. van den Brink	ECN Hydrogen and Clean Fossil Fuels
Checked by: W.G. Haije	Issued: F.A. de Bruijn	

DOI: 10.1002/cssc.200800085

The Crucial Role of the K^+–Aluminium Oxide Interaction in K^+-Promoted Alumina- and Hydrotalcite-Based Materials for CO_2 Sorption at High Temperatures

Stéphane Walspurger,* Luciaan Boels, Paul D. Cobden, Gerard D. Elzinga, Wim G. Haije, and Ruud W. van den Brink[a]

CO_2-free hydrogen can be produced from coal gasification power plants by pre-combustion decarbonisation and carbon dioxide capture. Potassium carbonate promoted hydrotalcite-based and alumina-based materials are cheap and excellent materials for high-temperature (300–500 °C) adsorption of CO_2, and particularly promising in the sorption-enhanced water gas shift (SEWGS) reaction. Alkaline promotion significantly improves CO_2 reversible sorption capacity at 300–500 °C for both materials. Hydrotalcites and promoted hydrotalcites, promoted magnesium oxide and promoted γ-alumina were investigated by in situ analytical methods (IR spectroscopy, sorption experiments, X-ray diffraction) to identify structural and surface rearrangements. All experimental results show that potassium ions actually strongly interact with aluminium oxide centres in the aluminium-containing materials. This study unambiguously shows that potassium promotion of aluminium oxide centres in hydrotalcite generates basic sites which reversibly adsorb CO_2 at 400 °C.

Introduction

Power generation from coal with reduced CO_2 emissions can be achieved by using an integrated gasification combined cycle with CO_2 capture and storage in the near future. In CO_2 capture, transport and storage, it is currently the capture that accounts for the highest extra costs. Reduction of the efficiency penalty owing to CO_2 capture and abatement of the capital costs associated with the extra equipment are necessary. The sorption-enhanced reaction process (SERP) has attracted great interest because of the optimization of reaction yield and hydrogen purity.[1] Furthermore, it offers the opportunity to separate CO_2 from the fuel and eventually to capture it for long-term storage[2–4] or for its further use as a hydrogen carrier through methanol synthesis, for instance.[5] Process simulations have shown that SERP using the pressure swing adsorption mode has a high potential for lower efficiency penalties and may imply lower equipment costs at the same time.[6,7] Gasification products mainly consist of CO, which has to be converted into H_2 and CO_2 through the water gas shift reaction [Eq. (1)]. In sorption-enhanced water gas shift (SEWGS), the equilibrium of the reaction is shifted to the product side by removing one of the products using a sorbent.

$$H_2O + CO \rightleftharpoons H_2 + CO_2 \quad (\Delta H_{298}{}^0 = -41\ kJ\,mol^{-1}) \qquad (1)$$

With a CO_2 sorbent, the thermodynamic equilibrium is thus shifted to hydrogen production, which can be free from carbon in an ideal case. The development of such a process was started by Air Products in the 1990s.[1] The sorption-enhanced reaction was demonstrated at about 300–500 °C using clays (hydrotalcite $Mg_{1-x}Al_x(OH)_2(CO_3)_{x/2}\cdot n\,H_2O$) or Na_2O–alumina as CO_2 sorbent.[8,9] Attention has been focused especially on hydrotalcites because they display 1) relatively fast reversible adsorption/desorption rates, 2) a stable capacity for CO_2 during long-term cyclic experiments, 3) fairly good mechanical strength in high-pressure steam and 4) no interaction with the physically mixed water gas shift catalyst.

By using hydrotalcites as a sorbent, the process is operated successfully at temperatures between 350 and 450 °C in a pressure swing adsorption unit (pressure between 1 and 30 bars) on a bench scale (single column, height 2 m, diameter 38 mm, CACHET project) at the Energy Research Centre of the Netherlands (ECN).[10] In parallel with the bench-scale experiment, investigations on hydrotalcite and derivative materials are ongoing at the laboratory scale. Despite a few earlier studies on CO_2 sorption using hydrotalcite-based sorbents under water gas shift conditions,[8,9,11–13] the true nature of the species responsible for CO_2 reversible adsorption at such temperatures is still not well understood. In particular, the present study is focused on the role of alkaline promoters which have been earlier found to significantly increase the CO_2 sorption capacity of hydrotalcites.[5,14–16] Lee et al.[9] and Ebner et al.[16] have proposed models for adsorption mechanisms based on sorption isotherms, but the exact nature of the active species in CO_2 sorption at such high temperatures remains unknown. Particularly, hydrotalcites as acid–base materials[17] may contain sites with an optimal basic strength for CO_2 fixation at high temperature.

[a] *Dr. S. Walspurger, L. Boels, P. D. Cobden, G. D. Elzinga, Dr. W. G. Haije, Dr. R. W. van den Brink*
Hydrogen Production and Clean Fossil Fuels
Energy Research Centre of the Netherlands (ECN)
Westerduinweg 3, 1755LE, Petten (The Netherlands)
Fax: (+31) 224-56-8489
E-mail: walspurger@ecn.nl

Here, we aimed to elucidate the type of active species responsible for the CO_2 adsorption under water gas shift conditions. Our approach was based on a systematic study of "parent" materials of hydrotalcites, such as alumina and magnesium oxide and their potassium carbonate promoted forms, by comparison of their CO_2 capacities and thermal decomposition. Characterisation of these materials was performed by in situ X-ray diffraction (XRD) to check phase transformation and by IR spectroscopy to identify rearrangements that occur at high temperatures and the CO_2 adsorption mechanism. This study targeted a better understanding of the active species in CO_2 fixation for further optimisations by a rational design of the sorbent.

Results and Discussion

First, note that CO_2 fixation by a solid can be interpreted in terms of acid–base interaction. Hydrotalcites are included in acid–base materials that are extensively used in chemistry, from catalyst carriers[19,20] and host materials[21] to reusable catalysts in fine organic synthesis.[22–24] Abundant relevant data can be found in the literature on the evidence of unique acid–base properties[25–29] and on the enhancement of their basic character by alkaline promotion.[30,31]

Reversible Capacity and Carbonate Decomposition

Note that the hydrotalcites used in this study were first calcined at 400 °C, promoted by potassium carbonate by incipient wetness and then dried at 120 °C. In the following discussion the material is noted as HT* (see Experimental Section). Activated hydrotalcite $Mg_{1-x}Al_x(OH)_2(CO_3)_{x/2}{\cdot}n\,H_2O$ and their potassium carbonate promoted forms were first investigated for their reversible CO_2 adsorption in the presence of a high partial pressure of steam at 400 °C. Indeed, it was found earlier that the presence of steam in the gas stream has a significant effect on the capacity for CO_2.[13,32,33] Increasing the steam/CO_2 ratio facilitates a quick and efficient desorption and has a positive influence on the adsorption capacity as demonstrated recently.[33] Moreover, it is worth to test sorbents under conditions that are close to the real SEWGS application.[10]

Figure 1 shows the typical breakthrough curves for various potassium carbonate loadings on hydrotalcite (HT*). Non-promoted hydrotalcite showed a low reversible capacity under our experimental conditions. Clearly, modification by potassium carbonate strongly enhances CO_2 capacity of HT* as demonstrated earlier.[13] Reversible capacities for other materials were measured using the same method, and the results after the third cycle are presented together with nitrogen sorption results in Table 1. Note that generally there was only a very small difference between the second and third cycles, and longer tests carried out for some of these materials confirmed that the capacity does not vary significantly after the third cycle under these conditions.

These experiments confirm that there exists an optimal loading of K_2CO_3 on hydrotalcites and that the surface area drops dramatically at high loadings.[34] The same conclusion could be drawn from the results obtained with promoted aluminas. Although unpromoted γ-alumina did not show any affinity for CO_2 under the experimental conditions, it clearly appeared that potassium carbonate promotion allows CO_2 fixation despite a pronounced drop in specific surface area. The lower surface areas found at high K_2CO_3 loadings are most probably caused by pore or surface blockage owing to the formation of bulk K_2CO_3 aggregates as revealed by scanning electron microscopy (SEM) images (Figure 2).

The typical platelet-like hydrotalcite particles of the initial material are partially covered by some needle-shaped material after impregnation with potassium carbonate. In full agreement with the recent contribution of Rodrigues and co-workers on potassium-modified hydrotalcite,[35] small needle-shaped aggregates can also be clearly seen on the γ-alumina surface in a very similar way. Although energy-dispersive X-ray (EDX) analysis did not allow a definitive answer, it may be assumed that the needles are hydrates of potassium carbonate which

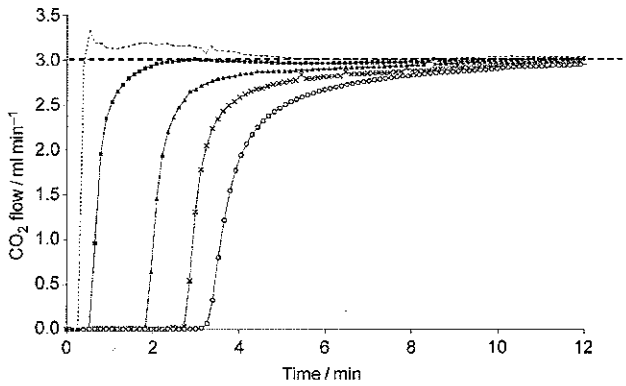

Figure 1. CO_2 breakthrough curves in sorption capacity measurement using 5.8% CO_2, 10.7% H_2O, and N_2 balance as gas feed for the adsorption step at 400 °C, 1 bar total pressure: (----) blank, (■) K_0HT*, (▲) K_5HT*, (+) K_{11}HT* and (○) K_{22}HT*.

Table 1. CO_2 reversible sorption capacities at 400 °C for hydrotalcite, potassium carbonate promoted hydrotalcites and other selected materials along with their specific surface area (SSA).[a]

Sample	K_2CO_3 loading [wt%]	BET SSA [$m^2\,g^{-1}$]	CO_2 rev. sorp. cap. [mmol g^{-1}][b]	Mg/Al ratio
K_0HT*	0	48	0.06	2.33
K_5HT*	5	41	0.19	2.33
K_{11}HT*	11	40	0.30	2.33
K_{22}HT*	22	18	0.37	2.33
K_0AO	0	256	0	0
K_5AO	5	–	0.01	0
K_{11}AO	11	–	0.07	0
K_{22}AO	22	113	0.27	0
K_{44}AO	44	–	0.26	0
K_0MO	0	86	0	∞
K_{22}MO	22	6	0.06	∞
K_2CO_3	100	–	0	–

[a] HT = hydrotalcite, AO = alumina, MO = magnesium oxide. [b] CO_2 reversible sorption capacity at 400 °C.

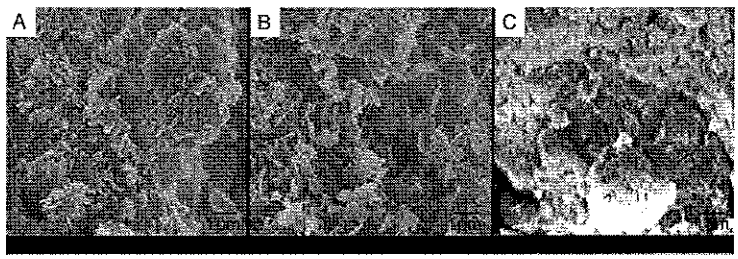

Figure 2. SEM images of A) unpromoted hydrotalcite, B) 22 wt% K_2CO_3-promoted hydrotalcite and C) 22 wt% K_2CO_3-promoted γ-alumina.

have been reported as needle-shaped crystalline material in early studies.[36] It is clear that at least part of the material deposited on the surface is responsible for the increased CO_2-sorption capacities for all those materials. In contrast, note that commercial bulk potassium carbonate as well as magnesium oxide and other magnesium oxide precursors (Brucite $Mg(OH)_2$ and hydromagnesite $Mg_5(CO_3)_4(OH)_2{\cdot}4H_2O$) did not show any CO_2 reversible adsorption capacity under the experimental conditions used. Moreover, potassium carbonate promoted magnesium oxide showed only a very low reversible CO_2-adsorption capacity compared to the aluminium oxide based materials. Hence, it seems that the interaction between the γ-alumina surface or aluminium oxide centres and potassium carbonates does play a key role in the formation of sites[37–39] that do actively and reversibly fix carbon dioxide under the experimental conditions used.

Temperature-programmed desorption (TPD) studies were carried out to analyse the decomposition of carbonates for various samples. The released CO_2 was analysed by mass spectrometry for hydrotalcites and aluminas with increasing potassium carbonate loadings and for a potassium carbonate promoted magnesium oxide (Figure 3).

For unpromoted hydrotalcite, the desorption profile under standard conditions (heating in a flow of nitrogen (50 mL min^{-1}) to 900 °C at a rate of 10 °C min^{-1}) showed a maximum at about 400 °C with a rather narrow shape, although a small tail was present at higher temperature corresponding to the decomposition of carbonates at higher temperature. Although the curve was clearly broadened as a result of the higher concentration of carbonate in the hydrotalcite promoted with 5 wt% potassium carbonate, the peak corresponding to the decomposition temperature was not shifted towards higher temperatures. More interestingly, with higher loadings the maximum of the decomposition peak shifted toward higher temperature while its profile was significantly broadened. Note that at 22 wt% K_2CO_3, a significant second CO_2 peak was observed at 830 °C probably due to the presence of bulk carbonate at the surface of the mixed oxide (originally hydrotalcite). Although commercial bulk potassium carbonate started to decompose above 900 °C under these experimental conditions, it can be assumed that bulk potassium carbonate deposited on the surface of the solid (as observed by SEM) is responsible for the CO_2 release at such a high temperature. The corresponding experiments on γ-alumina and promoted γ-alumina are depicted at the centre of Figure 3. As expected, unpromoted γ-alumina did not show any carbonate decomposition at high temperature and only a minor amount of residual CO_2 is desorbed between 100 and 200 °C. An increase in the amount of potassium carbonate on the surface led to an increased amount of CO_2 released between 250 and 450 °C.

Interestingly, samples with an increased amount of potassium carbonate showed a gradual shift of the maximum corresponding to carbonate decomposition from 290 to 335 °C with a strong broadening of the temperature range at which CO_2 was released toward high temperatures. Furthermore the shift of the maximum decomposition peak toward higher temperature was confirmed in extra experiments with various heating rates (data not shown). Most probably, some carbonates more strongly bonded to the surface, which are formed at higher surface coverage, may be responsible for the modification of the TPD profile. Finally, it is of greatest interest to compare the decomposition profile for potassium carbonate impregnated on various supports, namely alumina, hydrotalcite and magnesium oxide. In comparison to bulk potassium carbonate, it is clear that potassium carbonate impregnated on these supports undergoes a transformation that decreases the initial decomposition temperature of K_2CO_3. Apparently, alumina can destabilise potassium carbonate to a high extent as some CO_2 was already released at 250 °C. However the results from the thermal decomposition curves can hardly be directly correlated to the reversible CO_2-sorption properties shown in Table 1. In other words, it would be rather difficult to assign a specific group of carbonates responsible for the increased CO_2 reversible capacity on the basis of the decomposition of carbonates. Note that one can try to analyse the results from the decomposition of carbonates in terms of basic strength. Indeed, CO_2 as an acid probe is entrapped in carbonate form on the solid surface. The desorption of CO_2 may restore the initial basic site, and as a result the temperature of the decomposition of carbonates may reflect, to some extent, the bond strength be-

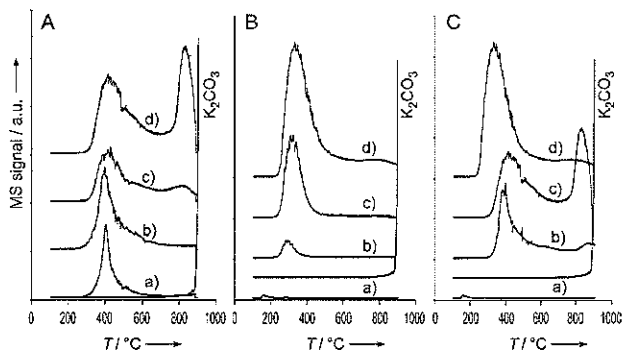

Figure 3. TPD profiles of CO_2 for A) a) K_0HT^*, b) K_5HT^*, c) $K_{11}HT^*$, d) $K_{22}HT^*$; B) a) K_0AO, b) K_5AO, c) $K_{11}AO$, d) $K_{22}AO$; and C) a) K_0AO, b) $K_{22}MO$, c) $K_{22}HT^*$, and d) $K_{22}AO$.

tween CO_2 and the basic site, or in other words, it may give insights to the basic strength of the surface sites. Following this concept, it appears from TPD profiles that the higher the carbonate loading the more sites of higher basic strength are formed on the surface, confirming the results found by Wang et al.[30,38,40] It might be that a population of sites with appropriate basic strength is specifically involved in the reversible CO_2 sorption at 400 °C. In situ structural analysis and spectroscopic investigations were therefore carried out to identify rearrangements taking place in the sorbent under working conditions.

Hydrotalcite Structural Rearrangement During CO_2 Capture

Variable-temperature in situ XRD experiments were performed with hydrotalcites and promoted hydrotalcite in the presence of steam (3 vol%) both in the presence and absence of carbon dioxide (12 vol%; Figure 4). Unpromoted hydrotalcite (K_0HT*) and 22 wt% potassium carbonate promoted hydrotalcite (K_{22}HT*) were heated gradually to 500 °C in the chosen gas stream, and diffraction patterns were recorded at various temperatures. Figure 4A displays the pattern obtained for K_0HT* in a nitrogen/steam mixture. Note that the diffraction patterns taken at room temperature showed the hydrotalcite crystalline structure that has been reformed (reconstructed) after calcination at 400 °C with subsequent impregnation with water at room temperature and drying at 120 °C overnight (Experimental Section).

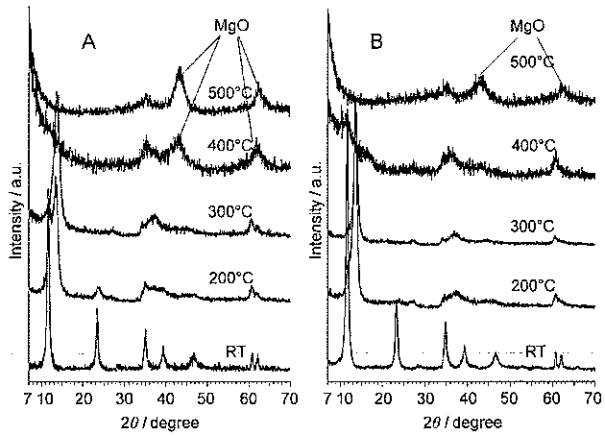

Figure 4. In situ XRD profiles for A) K_0HT* at variable temperatures in steam/nitrogen and B) K_0HT* at variable temperatures in steam/nitrogen/CO_2.

The well known decomposition of the hydrotalcite crystalline phase corresponding to the collapse of the layered structure is clearly observed together with the formation of small crystals of magnesium oxide,[41–44] although neither the $MgAl_2O_4$ spinel form (at high temperature) nor crystalline magnesium carbonate could be observed.[12] The temperature dependence of the crystalline rearrangement was only slightly different in the other experiments. With the addition of CO_2 to the gas stream, crystalline magnesium oxide appeared only at temperatures over 400 °C (above 300 °C in the absence of CO_2) for both unpromoted hydrotalcite (Figure 4B) and K_2CO_3-promoted hydrotalcite. In the latter case, with CO_2 in the stream, crystalline potassium carbonate was also observed during the experiment. Remarkably the main differences were observed while cooling the samples to room temperature in a fixed gas stream after heat treatment at 500 °C (Figure 5 and Figure 6).

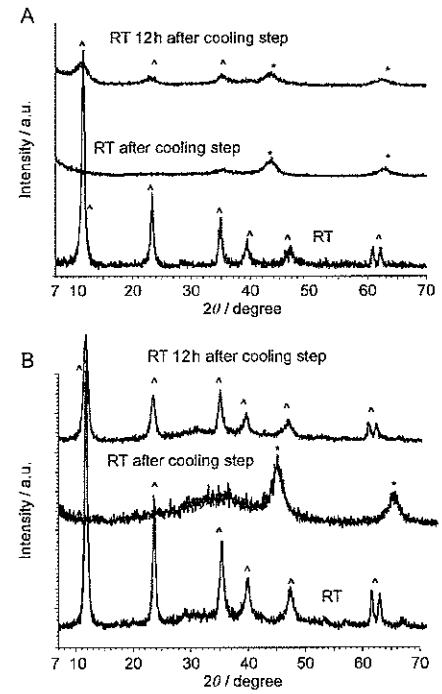

Figure 5. In situ XRD profiles in a stream of water/nitrogen for A) K_0HT* and B) K_{22}HT* at room temperature before heating, after heating at 500 °C and 12 h after heating at 500 °C. Crystalline hydrotalcite (^), MgO (*).

Indeed, samples in permanent contact with CO_2 (Figure 6) did not recrystallise to the hydrotalcite structure contrary to the samples that were flushed with nitrogen/steam where the memory effect of activated hydrotalcite was confirmed.[45]

CO_2 might help to stabilise some carbonate species at the surface which are poorly crystalline or non-crystalline, and thus it might hinder the reformation of hydrotalcite. In addition, it seems that potassium-promoted hydrotalcite is reconstructed faster than the unpromoted hydrotalcite in a nitrogen/steam stream (Figure 5A and B).

Surface Rearrangement During CO_2 Capture

In situ diffuse reflectance infrared Fourier transformed spectroscopy (DRIFTS) studies were carried out to identify the rearrangements involved in the solids at variable temperature (room temperature to 400 °C) in the presence of steam. The spectra in the 800–2000 cm^{-1} range obtained from unpromoted hydrotalcite, 22 wt% K_2CO_3-promoted hydrotalcite, γ-alumina and 22 wt% K_2CO_3-promoted γ-alumina are shown in Figures 7A–D, respectively. Before the heat treatment, a broad ab-

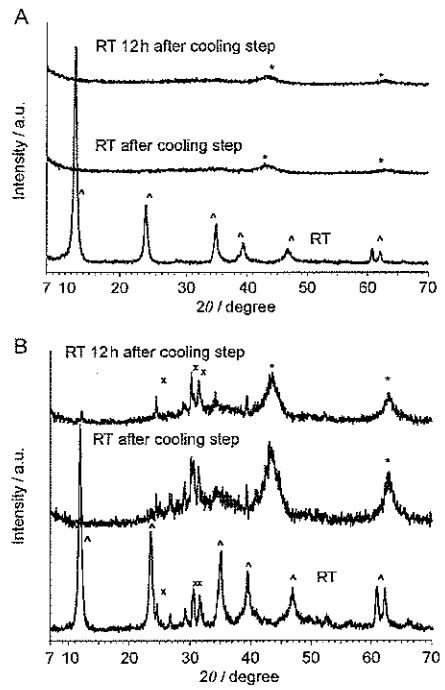

Figure 6. In situ XRD profiles in a stream of water/nitrogen + CO_2 for A) K_6HT^* and B) $K_{22}HT^*$ at room temperature before heating, after heating at 500 °C and 12 h after heating at 500 °C. Crystalline hydrotalcite (^), MgO (*) and K_2CO_3 (×).

sorption band is observed at 1655 cm^{-1} for all samples which is typical of the O–H bending mode of water.[25,46–48] Accordingly, this band disappears after thermal treatment at temperatures over 100 °C and reappears after rehydration of the sample at room temperature (data not shown). Note at this point that this band might also hint at the presence of bicarbonate species at low temperature which are known to decompose at rather low temperatures.[25,34]

The unpromoted hydrotalcite sample exhibited a strong and broad absorption band between 1400 and 1600 cm^{-1}. As the temperature is increased, there are clearly two maxima appearing at 1535 cm^{-1} and 1430 cm^{-1} (Figure 7A). These bands are generally assigned to ν_3 asymmetric stretching of carbonate groups.[25,47–51] The splitting is most probably caused by the rearrangement of surface carbonates that involves a lowering of their symmetry. According to Busca and Lorenzelli,[52] the splitting $\Delta\nu = 105$ cm^{-1} can be assigned to bidentate carbonates in this case, because the polarisation might be rather low for Mg-Al atoms. For the 22 wt% K_2CO_3-promoted hydrotalcite (Figure 7B), band splitting also occurs when the temperature is increased. Between 200 and 400 °C, there are two broad bands peaking at 1560 and 1370 cm^{-1} which correspond to the ν_3 vibrational mode of carbonate groups. Strikingly, the splitting is increased to $\Delta\nu = 190$ cm^{-1} denoting a stronger perturbation of the symmetry in carbonate groups as is confirmed by the appearance of the band at 1060 cm^{-1}, which is usually IR-inactive for symmetric carbonates. The main reason for this significant change may be the close interaction of surface carbonates with potassium ions provided by potassium carbonates. The band at 1430 cm^{-1} and the weak absorption band at 1740 cm^{-1} maximised at 400 °C can be unambiguously assigned to the vibration frequencies ν_3 and $2\nu_2$ (harmonic signal of ν_2, usually found at 870–880 cm^{-1}), respectively, of bulk potassium carbonate present in a large amount, in agreement with the observation made by TPD and SEM[53] studies.

In contrast, experiments on non-promoted γ-alumina (Figure 7C) showed that no carbonates were present on the surface at high temperature. At room temperature in the presence of steam and residual CO_2 from the atmosphere, bands were observed at 1655, 1520 and 1410 cm^{-1} corresponding most probably to surface bicarbonates.[54]

More interestingly, 22 wt% K_2CO_3-promoted γ-alumina showed a very clear picture on rearrangement of surface carbonates occurring at elevated temperature (Figure 7D). Two bands peaking at 1560 and 1362 cm^{-1} ($\Delta\nu = 198$ cm^{-1}) corresponds to ν_3 stretching frequencies for bidentate carbonates. The second band is rather large probably because of the presence of some bulk potassium carbonate with its typical single ν_3 frequency around 1430 cm^{-1}. Furthermore, the broadening of the bands may be explained by the presence of K-O-(CO)-O-Al species which usually exhibit a split ν_3 frequency and ν_1 at 1550, 1420 and 1095 cm^{-1}, respectively.[55,56] These species have previously been invoked to rationalize the enhanced basic strength of alkali-promoted aluminium oxides.[38,57,58]

Hence, the observed similarities between hydrotalcites and K_2CO_3-promoted γ-alumina may be of the utmost importance for the comprehension of the promoting mechanism. Carbonates provided by the addition of K_2CO_3 are rearranged at the surface as proved by the splitting of the ν_3 frequency for both materials. Moreover, by comparison of the splitting values observed for promoted hydrotalcite and promoted γ-alumina it clearly appears that the symmetry of the carbonates may be affected in a similar way. Thus, it is clear that Al centres play a major role in the destabilisation of potassium carbonate and may be at the origin of the increased CO_2 capacity observed in our experiments at 400 °C in agreement with previous reports.

Conclusions

Hydrotalcites, potassium carbonate promoted hydrotalcite and potassium carbonate promoted γ-alumina have been proved to be excellent materials for in situ CO_2 capture during the water gas shift process (SEWGS). Significant enhancement of CO_2 capacity can be achieved by alkaline promotion of the sorbents. We have unambiguously demonstrated that potassium carbonate is destabilized or transformed at the surface of metal oxides and particularly γ-alumina and hydrotalcites. Although no new carbonate structures or species could be identified by in situ XRD studies, we showed that fixed CO_2 at 300–500 °C hinders the reconstruction of hydrotalcites at room temperature most probably because of the formation of carbonate species. Moreover, the in situ DRIFTS study confirmed that rearrangement of surface carbonates occurs at high temperature and that the interaction between aluminium oxide centres and potassium carbonate plays a crucial role in the formation of

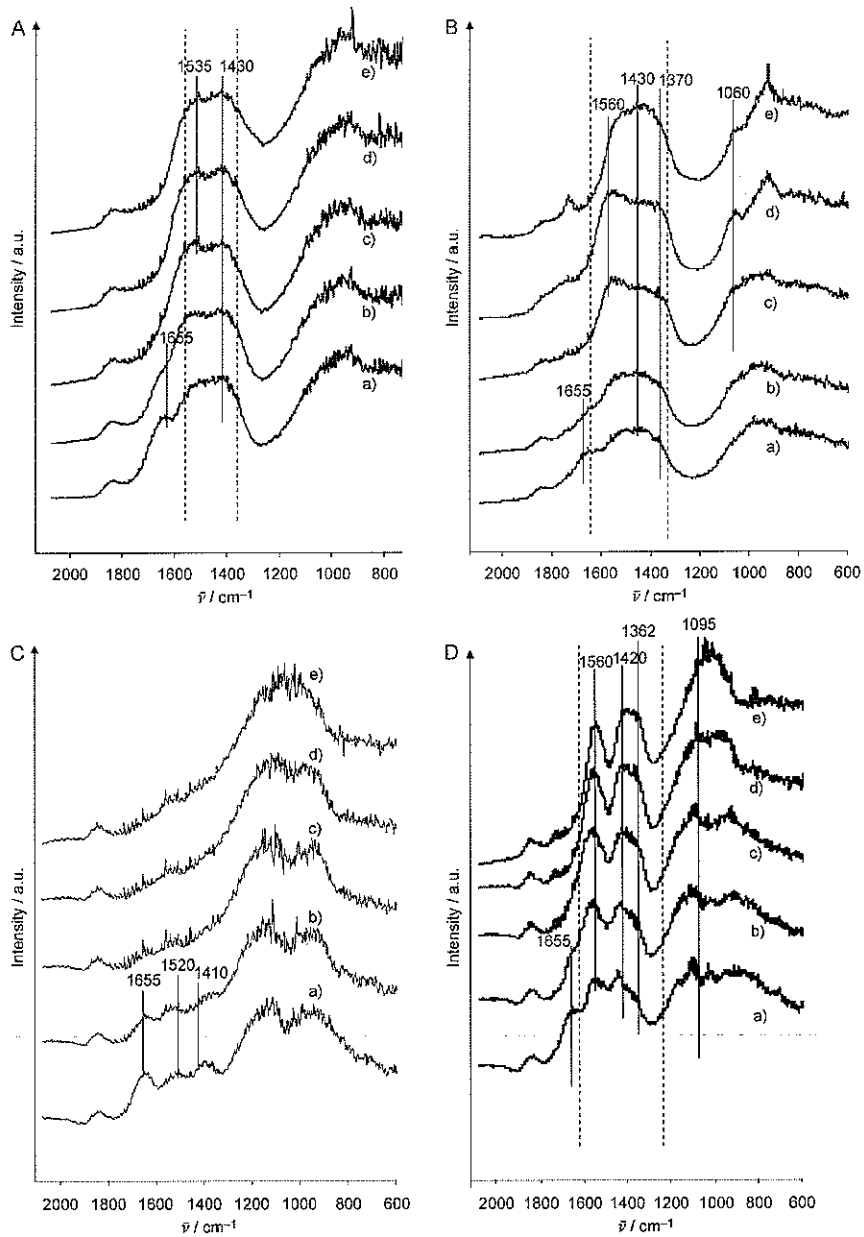

Figure 7. DRIFT spectra of A) K_0HT^*, B) $K_{22}HT^*$, C) K_0AO and D) $K_{22}AO$ in the carbonate region at room temperature in nitrogen/steam stream at a) room temperature, b) 100 °C, c) 200 °C, d) 300 °C, and e) 400 °C. Kubelka Munk intensities are reported.

active sites (strongly basic) for CO_2 capture at 300–500 °C. These findings are furthermore corroborated by the very low sensitivity of magnesium oxide to potassium promotion.

Experimental Section

Synthesis of hydrotalcite-based materials: The method was based on co-precipitation and adapted from a reported procedure.[18] Hydrotalcite (HT) with a molecular formula of $Mg_{0.70}Al_{0.30}(OH)_2(CO_3)_{0.15}\cdot n H_2O$ was synthesized as follows: Na_2CO_3 (p.a., Merck; 11 g) was dissolved in deionised water (200 mL) at 65 °C. While stirring, a solution of $Mg(NO_3)_2\cdot 6H_2O$ (p.a., Merck; 83 g, 0.32 mol) and $Al(NO_3)_3\cdot 9H_2O$ (52 g, 0.14 mol; p.a., Merck) in deionised water (450 mL) was added to the Na_2CO_3 solution at a constant rate of 9 mL min^{-1} using a peristaltic pump. The addition of the salt solution immediately led to the formation of a white precipitate. To prevent a drop in pH to below 8.5, automated addition of 3 M NaOH solution (p.a., Merck) was implemented. After the addition of all of the Mg/Al solution, the reaction mixture was kept at 65 °C and pH 8.5 for 21 h. Finally, the suspension was filtered, washed with deionised water (5× 1000 mL) at 55 °C and the residue was dried at 120 °C for 22 h. Samples of HT were activated by calcination in air at 400 °C for 4 h. Calcined samples (HT*) were promoted with 5, 11 and 22 wt% K_2CO_3 (p.a., Merck) by incipient wetness impregnation and dried overnight at 120 °C. These samples are denoted as K_xHT^* (K_x stands for the amount of K_2CO_3 in wt%).

Potassium modification of γ-alumina: γ-Al_2O_3 with a surface area of 328 m^{2}g^{-1} (Al-4170P, Engelhard) was used for the preparation of the potassium carbonate promoted alumina. The material was first dried at 80 °C overnight, and samples were promoted with 5, 11, 22 and 44 wt% K_2CO_3 by incipient wetness impregnation. Finally, the samples were dried at 120 °C for 22 h. For comparison purposes, a sample of potassium-free alumina was wetted and dried as described above. These samples are denoted as K_xAO (K_x stands for the amount of K_2CO_3 in wt%).

Potassium modification of magnesium oxide: MgO (>99%, Aldrich) and $Mg(OH)_2$ were used for the preparation of potassium carbonate promoted magnesium oxide. The magnesium oxide precursor was first dried at 80 °C overnight and was promoted with 22 wt% K_2CO_3 by incipient wetness impregnation. A reference sample was impregnated with pure water. Finally, the samples were dried at 120 °C for 22 h. These samples are denoted as K_xMO (K_x stands for the amount of K_2CO_3 in wt%).

Analytical methods: For analytical purposes and reproducibility, the materials were sieved into particles of sizes between 212 and 425 μm. Nitrogen adsorption was carried out at low temperature (−196 °C) in an AMI-200 (Altamira Instruments) designed for automated chemi-/physisorption. The samples were first treated at

150 °C for 10 h in a nitrogen flow, and the specific surface area (SSA) was then determined with the Brunauer–Emmet–Teller (BET) plot. With the same instrument, temperature-programmed desorption coupled with mass spectrometry (TPD) measurements were carried out. Typically, a sample of 180–250 mg was heated at 200 °C for 2.5 h. After cooling to 100 °C, the sample was heated in a flow of nitrogen (50 mL min^{-1}) to 900 °C at a rate of 10 °C min^{-1}, while continuously monitoring ions with m/z corresponding to H_2, CH_4, H_2O, $CO+N_2$, O_2 and CO_2.

The CO_2 capacity at 400 °C was estimated using the same setup and a modified procedure involving 1) heating the material in a flow of nitrogen saturated with water (at 47 °C corresponding to 107 mbars) at 400 °C during 1 h to remove any remaining CO_2 from synthesis and storage in atmosphere, 2) adsorption of CO_2 with a gas mixture containing 5.8% CO_2, 10.7% H_2O and balance N_2 for 45 min, and 3) desorption step in which a flow of nitrogen saturated with water (at 47 °C corresponding to 107 mbars) flushes the sample at 400 °C for one hour. In total, three adsorption/desorption cycles were performed, while the CO_2 concentration at the outlet was continuously monitored using the mass spectrometer. A blank experiment was performed using SiC sieved particles, which is a non-absorbing material.

In situ variable-temperature X-ray diffraction (VT-XRD) was performed in a controlled atmosphere in a Bruker AXS D8 Advance diffractometer with $Cu_{K\alpha}$ radiation, powered by a Kristallflex K760 generator at 40 kV and 40 mA. The scattering intensity was registered with an energy dispersive Sol-X detector (Bruker AXS) in the range $5° < 2\theta < 80°$. The samples were heated at 20 °C min^{-1} to the desired temperatures, and acquisition was started after 30 min equilibration. Scanning electron microscopy (SEM) was performed using an ultrahigh-vacuum JEOL scanning electron microscope (JSM-6330F) equipped with energy dispersive X-ray analyzer (EDX). Prior to analysis, the samples were sputter-coated with platinum. Diffuse reflectance infrared Fourier transform (DRIFT) spectroscopy was performed on a Biorad JT-1234 apparatus. The spectra were recorded while continuously flushing a special hot cell with controlled atmosphere.

Acknowledgements

We gratefully acknowledge financial support from the CATO-1 project and the Dutch Ministry of Economic Affairs. We thank Soledad Van Eijk and Özlem Pirgon-Galin for their assistance and fruitful advice.

Keywords: adsorption · basicity · CO_2 capture and storage · potassium · water gas shift

[1] S. Sircar, C. A. M Golden, US Patent 6322612, **2001**.
[2] *IEA Prospects for CO_2 Capture and Storage*, International Energy Agency, Paris, **2004**.
[3] B. Metz, H. C. Coninck, *CO_2 Capture and Storage: A Future for Coal?*, ECN policy study available at http://www.ecn.nl/publicaties/default.aspx?nr=ECN-B-07-020.
[4] C. Gough, *Int. J. Greenhouse Gas Control* **2008**, *2*, 155.
[5] G. A. Olah, A. Goeppert, G. K. S. Prakash, *Beyond Oil and Gas: The Methanol Economy*, Wiley-VCH, Weinheim, **2006**.
[6] J. R. Hufton, S. Mayorga, S. Sircar, *AIChE J.* **1999**, *45*, 248.
[7] M. C. Carbo, D. Jansen, J. W. Dijkstra, R. W. van den Brink, A. H. M. Verkooijen, *Pre-Combustion Decarbonisation in IGCC: Abatement of Both Steam Requirement and CO_2 Emissions*, ECN publication, **2007**, http://www.ecn.nl/publications/default.aspx?nr=ECN-M-07-055.
[8] K. B. Lee, A. Verdooren, H. S. Caram, S. Sircar, *J. Colloid Interface Sci.* **2007**, *308*, 30.
[9] K. B. Lee, M. G. Beaver, H. S. Caram, S. Sircar, *AIChE J.* **2007**, *53*, 2824.
[10] V. White, *CACHET 1st Workshop* (Athens, Greece), **2007**; available at http://www.cachetco2.eu/publications/conf_pubs.html.
[11] Z. Yong, V. Mata, A. E. Rodrigues, *Ind. Eng. Chem. Res.* **2001**, *40*, 204.
[12] N. D. Hutson, S. A. Speakman, E. A. Payzant, *Chem. Mater.* **2004**, *16*, 4135.
[13] H. T. J. Reijers, S. E. A. Valster-Schiermeier, P. D. Cobden, R. W. van den Brink, *Ind. Eng. Chem. Res.* **2006**, *45*, 2522.
[14] Y. Ding, E. Alpay, *Chem. Eng. Sci.* **2000**, *55*, 3461.
[15] S. Mayorga, S. Weigel, T. R. Gaffney, J. R. Brzozowski, US Patent 6,280,503B1, **2001**.
[16] A. D. Ebner, S. P. Reynolds, J. A. Ritter, *Ind. Eng. Chem. Res.* **2006**, *45*, 6387.
[17] K. Tanabe, H. Hattori, T. Yamaguchi, T. Tanaka, *Acid-Base Catalysis, Proceedings of the International Symposium on Acid–Base Catalysis, Sapporo*, VCH, Weinheim, **1989**.
[18] F. Cavani, F. Trifirò, A. Vaccari, *Catal. Today* **1991**, *11*, 173.
[19] K. O. Christensen, D. Chen, R. Lodeng, A. Holmen, *Appl. Catal. A Gen.* **2006**, *314*, 9.
[20] V. Rives, *Layered Double Hydroxides: Present and Future*, Nova Science, New York, **2001**.
[21] S. P. Newman, W. Jones, *New J. Chem.* **1998**, *22*, 105.
[22] J. C. A. A. Roelofs, A. J. Dillen, K. P. de Jong, *Catal. Today* **2000**, *60*, 297.
[23] J. I. Di Cosimo, C. R. Apesteguia, M. J. L. Gines, E. Iglesia, *J. Catal.* **2000**, *190*, 261.
[24] M. J. Climent, A. Corma, S. B. A. Hamid, S. Iborra, M. Mifsud, *Green Chem.* **2006**, *8*, 524.
[25] M. Del Arco, C. Martin, I. Martin, V. Rives, R. Trujillano, *Spectrochim. Acta Part A* **1993**, *49A*, 1575.
[26] J. Shen, J. M. Kobe, Y. Chen, J. A. Dumesic, *Langmuir* **1994**, *10*, 3902.
[27] J. Shen, T. Mai, C. Hu, *J. Solid State Chem.* **1998**, *137*, 295.
[28] E. Lima, M. Laspéras, L. C. de Ménorval, D. Tichit, F. Fajula, *J. Catal.* **2004**, *223*, 28.
[29] J. I. Di Cosimo, V. K. Diez, M. Xu, E. Iglesia, C. R. Apesteguia, *J. Catal.* **1998**, *178*, 499.
[30] Y. Wang, X. W. Han, A. Ji, L. Y. Shi, S. Hayashi, *Microporous Mesoporous Mater.* **2005**, *77*, 139.
[31] S. Abello, F. Medina, D. Tichit, J. Perez-Ramirez, X. Rodríguez, J. E. Sueiras, P. Salagre, Y. Cesteros, *Appl. Catal. A Gen.* **2005**, *281*, 191.
[32] S. Abello, J. Perez-Ramirez, *Microporous Mesoporous Mater.* **2006**, *96*, 102.
[33] M. K. RamReddy, Z. P. Xu, G. Q. Lu, J. C. Diniz da Costa, *Ind. Eng. Chem. Res.* **2008**, *47*, 2630.
[34] J. I. Yang, J. N. Kim, *Korean J. Chem. Eng.* **2006**, *23*, 77.
[35] E. L. G. Oliveira, C. A. Grande, A. E. Rodrigues, *J. Sep. Purif. Tech.* **2008**, *62*, 137.
[36] A. Pabst, *Am. Mineral.* **1930**, *15*, 69.
[37] T. Horiuchi, H. Hidaka, T. Fukui, Y. Kubo, M. Horio, K. Suzuki, T. Mori, *Appl. Catal. A Gen.* **1998**, *167*, 195.
[38] Y. Wang, J. H. Zhu, W. Y. Huang, *Phys. Chem. Chem. Phys.* **2001**, *3*, 2537.
[39] A. G. Okunev, V. E. Sharonov, A. V. Gubar, I. G. Danilova, E. A. Paukshtis, E. M. Moroz, T. A. Kriger, V. V. Malakhov, Y. I. Aristov, *Russ. Chem. Bull.* **2003**, *52*, 359.
[40] T. Yamaguchi, Y. Wang, M. Komatsu, M. Ookawa, *Catal. Surv. Jpn.* **2002**, *5*, 81.
[41] F. Rey, V. Fornes, J. M. Rojo, *J. Chem. Soc. Faraday Trans.* **1992**, *88*, 2233.
[42] M. L. Valcheva-Traykova, N. P. Davidova, A. H. Weiss, *J. Mater. Sci.* **1993**, *28*, 2157.
[43] J. C. A. A. Roelofs, J. A. Bokhoven, A. J. Dillen, J. W. Geus, K. P. de Jong, *Chem. Eur. J.* **2002**, *8*, 5571.
[44] T. Stanimirova, T. Hibino, V. Balek, *J. Therm. Anal. Calorim.* **2006**, *84*, 473.
[45] J. Pérez-Ramírez, S. Abello, N. M. van der Pers, *Chem. Eur. J.* **2007**, *13*, 870.
[46] Y. Kim, W. Yang, P. K. T. Liu, M. Sahimi, T. T. Tsotsis, *Ind. Eng. Chem. Res.* **2004**, *43*, 4559.
[47] J. T. Kloprogge, *The Application of Vibrational Spectroscopy to Clay Minerals and Layered Double Hydroxides, CMS Workshop Lectures, Vol. 13* (Ed.: J. T. Kloprogge), The Clay Mineral Society, Aurora, **2005**, pp. 203–238.

[48] R. L. Frost, B. J. Reddy, *Spectrochim. Acta Part A Mol. and Bimol. Spectr.* **2006**, *65*, 553.
[49] T. Hibino, Y. Yamashita, K. Kosuge, A. Tsunashima, *Clays Clay Miner.* **1995**, *43*, 427.
[50] F. Prinetto, G. Ghiotti, R. Durand, D. Tichit, *J. Phys. Chem. B* **2000**, *104*, 11117.
[51] F. Millange, R. I. Walton, D. O'Hare, *J. Mater. Chem.* **2000**, *10*, 1713.
[52] G. Busca, V. Lorenzelli, *Mater. Chem.* **1982**, *7*, 89.
[53] R. A. Nyquist, R. O. Kagel, *Handbook of Infrared and Raman Spectra of Inorganic Compounds and Organic Salts, Vol. 4*, Academic Press, San Diego, **1997**.
[54] C. Morterra, A. Zecchina, S. Coluccia, A. Chiorino, *J. Chem. Soc. Faraday Trans. 1* **1977**, *73*, 1544.
[55] A. S. Berger, N. P. Tomilov, I. A. Vorsina, *Russ. J. Inorg. Chem.* **1971**, *16*, 42.
[56] A. Iordan, M. I. Zaki, C. Kappenstein, *J. Chem. Soc. Faraday Trans.* **1993**, *89*, 2527.
[57] S. C. Lee, B. Y. Choi, T. J. Lee, C. K. Ryu, Y. S. Ahn, J. C. Kim, *Catal. Today* **2006**, *111*, 385.
[58] S. C. Lee, J. C. Kim, *Catal. Surv. Asia* **2007**, *11*, 171.

Received: April 21, 2008
Published online on June 23, 2008

